Optimizing Power Beacon Placement in WET Systems via Self-Organizing Maps

Gabriel C. R. Morás, Marcelo Vinícius S. de Oliveira, Victoria D. P. Souto, and Richard D. Souza

***Abstract*— This paper proposes a novel solution that jointly optimizes PBs placement and energy beamforming, relying solely on statistical channel state information (SCSI). The proposed method integrates Self-Organizing Maps (SOMs) with K-means clustering, both unsupervised machine learning techniques, to derive a suboptimal yet effective placement of PBs. Simulation results demonstrate that the proposed strategy reduces the total system charging time by up to 87% compared to random PBs deployment and achieves a performance close to that of benchmarks assuming perfect CSI (PCSI). Furthermore, the results confirm that appropriate PBs placement enables the use of simpler hardware at the PB – specifically, by reducing the number of antennas required – without significant loss in system efficiency, making the proposed solution suitable for practical WET deployments.**

***Keywords*— Wireless energy transfer, Machine Learning, PBs Placement, Beamforming.**

I. INTRODUCTION

Wireless Energy Transfer (WET) has emerged as a pivotal technology for enabling the sustained operation of Internet of Things (IoT) devices, particularly in environments where conventional energy sources are unavailable or impractical. Its importance is especially evident in applications such as smart agriculture, industrial monitoring, and remote sensing, all of which demand continuous and reliable power delivery. In this context, radio frequency-based WET (RF-WET) offers a promising solution, enabling wireless energy transfer over considerable distances [1]–[3]. However, the efficiency of RF-WET systems is highly influenced by the spatial configuration of Power Beacons (PBs), which must be strategically deployed to ensure comprehensive coverage while minimizing propagation losses [4]–[6]. For the remainder of this paper, the term WET will be used to refer specifically to RF-WET.

The strategic placement of PBs plays a fundamental role in ensuring balanced energy distribution across WET systems. An uneven deployment, characterized by either an overconcentration or a shortage of PBs in specific areas, can result in inefficient energy delivery, increased charging durations, and potential interruptions in device operation, thereby threatening the feasibility of the target application [4], [5]. Therefore, in response to the challenges associated with optimal PB deployment in WET systems, several strategies have been proposed in recent literature. Specifically, in [4], the authors present a method for PB placement in scenarios where both sensor locations and channel state information (CSI) are unknown. The PBs, which transmit omnidirectionally, are positioned to maximize the average minimum energy received across the coverage area, thereby ensuring that even the most disadvantaged IoT device meets its quality of service (QoS) requirements. In [5], a wavelet-based approach using Daubechies functions is introduced to determine optimal PB positions in rechargeable sensor networks. This method leverages the scalability and localization properties of wavelets to enhance energy efficiency and coverage. A different perspective is offered in [6], where a greedy algorithm is employed to optimize both the placement and orientation of directional PBs. This technique, which does not require CSI, reduces system complexity and is particularly suitable for low-complexity IoT deployments. Finally, in [7], the authors focus on battery-less wireless sensor networks, proposing an algorithm for optimal PB placement and an integer linear programming model for adaptive power control. The aim is to reduce interference and minimize data transmission time while ensuring sufficient energy availability.

Motivated by the above, this work introduces a novel strategy for WET systems that aims to minimize the total charging time of IoT devices. This is achieved through the joint optimization of energy beamforming at the PBs and the placement of PBs, relying solely on statistical CSI (SCSI). To solve the proposed optimization problem, an innovative method is developed based on Self-Organizing Maps (SOMs), further refined using the K-means clustering algorithm, both of which are unsupervised machine learning (ML) techniques. Analog beamforming is adopted at the PBs due to its hardware simplicity and lower energy consumption when compared to digital or hybrid beamforming architectures [8], [9]. Moreover, it is important to highlight that, unlike prior works such as [4], [5], [7], this study considers PBs equipped with multiple antennas. Furthermore, in contrast to existing approaches [4]–[7], this work uniquely addresses the joint optimization of energy beamforming and PBs deployment.

The main contributions of this paper are: (i) It is shown that the proposed suboptimal placement of PBs reduces the total charging time by up to 87% in specific deployment scenarios,

Gabriel C. R. Morás, Marcelo Vinícius S. de Oliveira, and Victoria D. P. Souto, National Institute of Telecommunication (Inatel), Santa Rita do Sapucaí, MG, e-mail: {gabriel.gc@ges.inatel.br, marcelosatyro@mtel.inatel.br, victoria.souto@inatel.br}; Richard D. Souza, Federal University of Santa Catarina, Florianópolis, SC, e-mail: {richard.demo@ufsc.br}. This work has been funded by the following research projects: Brasil 6G Project with support from RNP/MCTI (Grant 01245.010604/2020-14), xGMobile Project code XGM-AFCCT-20XX-Y-ZZ-1 with resources from EMBRAPII/MCTI (Grant 052/2023 PPI IoT/Manufatura 4.0 and FAPEMIG Grant PPE-00124-23), SEMEAR Project supported by FAPESP (Grant No. 22/09319-9), SAMURAI Project supported by FAPESP (Grant 20/05127-2), Ciência por Elas with resources from FAPEMIG (Grant APQ-04523-23), Fomento à Internacionalização das ICTMGs with resources from FAPEMIG (Grant APQ-05305-23), Programa de Apoio a Instalações Multiusuários with resources from FAPEMIG (Grant APQ-01558-24), and Redes Estruturantes, de Pesquisa Científica ou de Desenvolvimento Tecnológico with resources from FAPEMIG (Grant RED-00194-23), and by CNPq (305021/2021-4 and 443974/2024-1). This work has also been supported by a master/doctoral scholarship from CAPES, CNPq, FAPEMIG, FAPESP, xGMobile/EMBRAPII/MCTI.

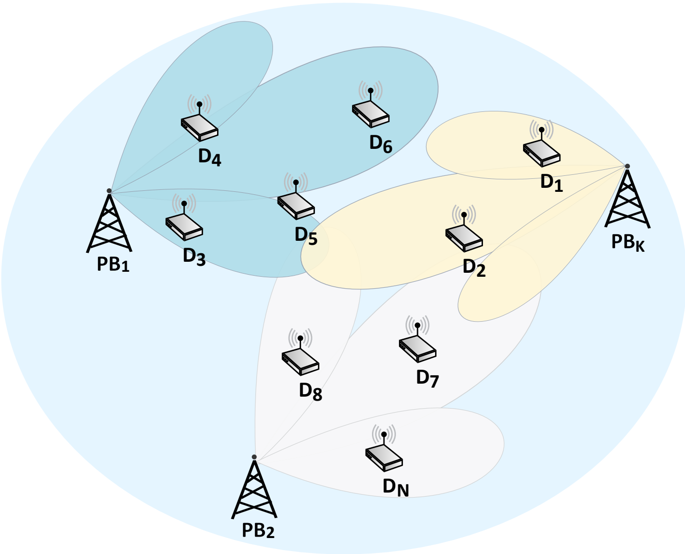

Fig. 1. System Model.

highlighting its effectiveness; and (ii) It is demonstrated that strategic placement of power beacons (PBs) enables the use of simpler hardware at the PBs — specifically, by reducing the number of antennas required — thereby mitigating the need for complex beamforming systems and reducing the overall system cost without significantly compromising performance.

II. System Model

In this work, we consider the system model illustrated in Figure 1, where a set of K PBs $\mathcal{P} = \{k = 1, 2, \ldots, K\}$ equipped with an uniform linear array (ULA) with M antennas charges a set of N IoT devices $\mathcal{I} = \{n = 1, 2, \ldots, N\}$. Additionally, in this paper, we consider the analog beamforming architecture and the beamsharing technique, which allows IoT devices to harvest energy while adjacent devices are being charged. Moreover, let $\mathbf{h}_{n,k} \in \mathbb{C}^{M\times 1}$ be the channel vector between the k-th PB and the n-th device modeled as a Rician fading defined as [10]

$$\mathbf{h}_{n,k} = \sqrt{\frac{\kappa_{n,k}}{1+\kappa_{n,k}}}\mathbf{h}_{n,k}^{\text{LoS}} + \sqrt{\frac{1}{1+\kappa_{n,k}}}\mathbf{h}_{n,k}^{\text{NLoS}}, \tag{1}$$

where $\mathbf{h}_{n,k}^{\text{LoS}} \in \mathbb{C}^{M\times 1}$ denotes the line-of-sight (LoS) component of the channel, $\mathbf{h}_{n,k}^{\text{NLoS}} \in \mathbb{C}^{M\times 1}$ is the non-LoS (NLoS) component of the channel modeled as a Rayleigh fading distribution, and $\kappa_{n,k}$ is the Rician factor quantifying the LoS-to-NLoS power ratio of the channels. In addition, the path loss for all links is modeled using the log-distance path loss model,

$$\gamma_{n,k} = \frac{\lambda^2}{16\pi^2 d_{n,k}^{\alpha_{n,k}}}, \tag{2}$$

where λ is wavelength, $d_{n,k}$ is the distance between the k-th PB and the n-th IoT device, and $\alpha_{n,k}$ is the path loss exponent.

The total power harvested by the n-th IoT device is

$$P_n = \sum_{k\in\mathcal{P}} \delta_{n,k}\gamma_{n,k}|\mathbf{w}_{n,k}\mathbf{h}_{n,k}^{\text{H}}|^2 + \sum_{\substack{j\in\mathcal{I}\\ j\neq n}}\sum_{k\in\mathcal{P}} \delta_{j,k}\gamma_{n,k}|\mathbf{w}_{j,k}\mathbf{h}_{n,k}^{\text{H}}|^2, \tag{3}$$

where the first term of refers to the power collected when the PB is pointed to the k-th device and the second term is related to the power collected by the k-th device while the PB is actively charging the j-th device. In addition, $\delta_{n,k} \in \{0, 1\}$ indicates which IoT device each PB is targeting. Specifically, if $\delta_{n,k} = 1$, the k-th PB is focusing its beamforming on the n-th device. The vector $\mathbf{w}_{n,k}$ denotes the analog beamforming vector of the k-th PB, targeting the the n-th device, with the constraint $||\mathbf{w}_{n,k}||^2 = P_{\text{T}}$, where P_{T} denotes the maximum transmission power of the PBs.

Finally, the total energy harvested by the n-th device is

$$\begin{aligned} E_n = &\sum_{k\in\mathcal{P}} \frac{t_{n,k}[\mathcal{L}_n(\delta_{n,k}\gamma_{n,k}|\mathbf{w}_{n,k}\mathbf{h}_{n,k}^{\text{H}}|^2) - \mu\Omega]}{1-\Omega} \\ &+ \sum_{\substack{j\in\mathcal{I}\\ j\neq n}}\sum_{k\in\mathcal{P}} \frac{t_{j,k}[\mathcal{L}_n(\delta_{j,k}\gamma_{n,k}|\mathbf{w}_{j,k}\mathbf{h}_{n,k}^{\text{H}}|^2) - \mu\Omega]}{1-\Omega}, \end{aligned} \tag{4}$$

where $t_{n,k}$ denotes the period of time that the k-th PB is focusing on the n-th IoT device, $\Omega = \frac{1}{1+e^{ab}}$. In addition, $\mathcal{L}_n(x)$ denotes the logistic function that characterizes the non-linear energy conversion behavior of the IoT devices' circuits, which is representative of practical systems, such as those developed by Powercast [11], and is defined as [10]

$$L_n(x) = \frac{\mu}{1+e^{-a(P_n(x)-b)}}, \tag{5}$$

where μ is the maximum energy that can be harvested.

III. Proposed Optimization Problem

The primary objective of this paper is to minimize the total charging time required to power a large number of IoT devices $\left(t_{\text{T}} = \sum_{n\in\mathcal{I}}\sum_{k\in\mathcal{P}}\delta_{n,k}t_n\right)$ by jointly optimizing the beamforming design at the PBs and the deployment strategy of the PBs. To this end, we formulate and aim to solve the following optimization problem.

$$\begin{aligned} \underset{\mathbf{w}_{n,k}, x_{\text{PB}_k}, y_{\text{PB}_k}, t_{n,k}}{\text{Minimize}} \quad & t_{\text{T}} = \sum_{n\in\mathcal{I}}\sum_{k\in\mathcal{P}}\delta_{n,k}t_{n,k} \\ \text{Subject to} \quad & E_n \geq E_{\text{min}} \quad \forall n \in \{1,\ldots,N\}, \\ & x_{\text{PB}_k}, y_{\text{PB}_k} \in [-R, R], \ \forall k \in \{1,\ldots,K\}, \\ & |w_{n,k,m}|^2 = \frac{P_T}{M}, \ \forall n, k, m, \\ & m \in \{1,\ldots,M\}, \end{aligned} \tag{6}$$

where E_{min} denotes the minimum energy constraints for the IoT devices, $|w_{n,k,m}|^2 = \frac{P_T}{M}$ is the analog beamforming constraint, and $(x_{\text{PB}_k}, y_{\text{PB}_k} \in [-R, R])$ denotes the constraint in terms of PB position, where R limits the system area.

As seen in (6), obtaining the optimal value of t_{T} relies on the assumption of perfect CSI (PCSI) at the PBs, which is generally unrealistic in practical applications. Consequently, following the approach in [12], the beamforming vector for each PB is designed using only SCSI, and is expressed as

$$\mathbf{w}_{n,k} = \sqrt{\frac{P_{\text{T}}}{M}}\left[\frac{h_{n,k,1}^{\text{LoS}}}{|h_{n,k,1}^{\text{LoS}}|}, \frac{h_{n,k,2}^{\text{LoS}}}{|h_{n,k,2}^{\text{LoS}}|}, \cdots, \frac{h_{n,k,M}^{\text{LoS}}}{|h_{n,k,M}^{\text{LoS}}|}\right]^T. \tag{7}$$

By incorporating the beamforming expression in (7) into (6), the optimization problem can be reformulated as follows:

$$\begin{aligned} \underset{x_{\mathrm{PB}_k}, y_{\mathrm{PB}_k}, t_{n,k}}{\text{Minimize}} \quad & t_{\mathrm{T}} = \sum_{n \in \mathcal{I}} \sum_{k \in \mathcal{P}} \delta_{n,k} t_{n,k} \\ \text{Subject to} \quad & E_n \geq E_{\min} \ \ \forall n \in \{1, \ldots, N\}, \\ & 0 \leq x_{\mathrm{PB}_k}, y_{\mathrm{PB}_k} \geq R, \ \forall k \in \{1, \ldots, K\}, \end{aligned} \tag{8}$$

From (8), it is evident that the integration of the beamsharing strategy significantly increases the complexity of the problem, making the derivation of a closed-form solution highly challenging. Furthermore, under the minimum energy requirement constraint imposed on the IoT devices, the total charging time is inherently affected by the energy harvested through neighboring influence, i.e., the energy harvested by a given IoT device when PBs are actively charging adjacent devices. Consequently, the spatial deployment of PBs has a direct impact on t_{T}. To address this, the next section presents a novel solution based on SOM technique to minimize t_{T}.

IV. Proposed Strategy Based on SOMs

To address the optimization problem defined in (8), this paper introduces a novel solution that utilizes SOMs enhanced by the K-means clustering technique, both of which are unsupervised ML methods. To facilitate a clearer understanding, the following subsection outlines the key characteristics of the employed ML techniques.

A. Self Organizing Maps

SOMs are a class of competitive neural networks specifically designed to project high-dimensional input data onto a lower-dimensional (typically two-dimensional) grid, while preserving the topological structure of the original data space. This topological preservation enables SOMs to capture spatial patterns and similarities within the data, making them particularly effective for clustering tasks and spatial pattern recognition [13], [14]. In the context of WET systems, SOMs are especially useful for organizing IoT devices based on factors such as geographic location, energy demand, and environmental conditions, thereby facilitating efficient resource allocation and system planning. Therefore, the training process of a SOM typically involves the following steps [13], [14]:

1. **Initialization:** A grid of neurons is initialized, each associated with a randomly generated weight vector.
2. **Input Mapping:** Each IoT device is represented as a feature vector (e.g., spatial coordinates, energy demand) and sequentially presented to the network.
3. **Best Matching Unit (BMU) Selection:** For each input vector, the neuron with the weight vector most similar to the input (typically measured by Euclidean distance) is identified as the BMU.
4. **Weight Adjustment:** The weight vectors of the BMU and its neighboring neurons are adjusted to move closer to the input vector. The magnitude of the adjustment is governed by a learning rate and a neighborhood function, both of which typically decrease over time.
5. **Convergence:** Over multiple iterations, the network gradually stabilizes, forming a topologically ordered map in which neurons represent clusters that reflect the spatial distribution of the IoT devices.

Through repeated iterations, SOMs progressively adapt to capture the intrinsic structure of the input data. This self-organization process facilitates meaningful clustering and spatial mapping [13], [14], which are particularly advantageous for applications such as managing IoT device deployments and optimizing the PBs placement in WET systems.

B. K-means

Although SOM groups similar data by preserving topological relationships, they do not explicitly define clusters, only neighborhood units. Consequently, to cluster the IoT devices, it becomes necessary to apply an additional clustering technique. Among the numerous available options, K-Means is extensively employed due to its conceptual simplicity, computational efficiency, and effectiveness in partitioning data into distinct and well-separated clusters [15], [16]. The standard procedure of the K-Means algorithm involves the following [15]:

1. **Initialize Cluster Centers (Centroids):** K initial centroids are chosen randomly or based on prior knowledge (e.g., from a SOM).
2. **Assign Data Points to the Nearest Centroid:** Each data point (e.g., an IoT device location) is assigned to the closest centroid based on Euclidean distance.
3. **Update Centroids:** The centroid of each cluster is recomputed as the mean of all points assigned to it.
4. **Convergence:** The process continues iteratively until centroids stabilize (i.e., there are minimal changes between iterations) or a stopping criterion is met.

C. Complete Proposed Solution

Motivated by the capabilities of the previously described ML techniques, this paper proposes a novel approach to minimize the total charging time (t_{T}). The proposed method aims to determine suboptimal placements of multiple PBs and to design their corresponding beamforming vectors based solely on SCSI. The key steps of the proposed solution are:

1. Initialize the set of uncharged IoT devices $\big(\mathcal{N}_{\mathrm{C}} = \{1, \ldots, N\}\big)$;
2. Initialize the device positions as data ($\mathbf{X}$);
3. Determine the best SOM hyperparameters, i.e., σ, which controls the neighborhood radius within which neurons around the BMU are updated, and ℓ, the learning rate, which controls the magnitude of weight updates during the training process;
4. Train the SOM considering the data defined in Step 2 and the best hyperparameters computed in Step 3;
5. Determine the clustering based on K-means considering the SOM weights computed in Step 4;
6. Define the PBs positions based on the centroids of the clusters defined in Step 5.
7. **While** $\big(\mathcal{N}_{\mathrm{C}} \neq \emptyset\big)$ **does:**
   - **7.1.** Each PB selects the IoT device closest to the PB, defining the charging order of the IoT devices based on Euclidean distance;

TABLE I
SIMULATION PARAMETERS.

Parameter	Variable	Value
Path loss exponent [17]	$\alpha_{n,k}$	2.7 $\forall n, k$
EH constant	μ	10.73 mW
Circuit constant [18]	a	5.365
Circuit constant [18]	b	0.2308
Carrier frequency [11]	f	915 MHz
PB transmission power [11]	P_{T}	3 W
Number of antennas at the PBs	M	4
Rician factor	$\kappa_{n,k}$	1.0 $\forall n, k$
Minimum energy requirement	$E_{\min}$	1 μJ
Number of PBs (clusters)	K	4
Maximum coverage radius	R	30 m
Number of IoT devices	N	20

7.2. Design the beamforming vector $\mathbf{w}_{n,k}$ for each PB based on (7) considering the IoT device allocated in the previous step;

7.3. Determine the power harvested by each IoT device based on (3);

7.4. Determine $t_{n,k}$ for the IoT devices $(\mathcal{N}_{\text{C}})$ allocated for each PB in Step 7.1, given by

$$t_{n,k} = \frac{(E_{\min} - E_n)(1 - \Omega)}{\mathcal{L}_n(P_n) - \mu\Omega}. \quad (9)$$

7.5. Compute E_n $\forall n \in \mathcal{N}_{\text{C}}$ based on (4) considering the minimum $t_{n,k}$ determined in the previous Step;

7.6. Verify if the device has reached its energy constraint ($E_{\min}$), remove the device from $\mathcal{N}_{\text{C}}$ and return to Step 7. Otherwise, return to Step 7;

V. RESULTS AND DISCUSSIONS

This section presents the simulation results obtained using the proposed solution described in Section IV.C. The evaluation is conducted in a scenario where multiple IoT devices are uniformly distributed over a two-dimensional plane, with their positions defined by coordinates (x_n, y_n). To assess the effectiveness of the proposed method, the following benchmark schemes are considered: (i) **PCSI:** This benchmark is based on the proposed framework, assuming perfect CSI at the PBs. Under this assumption, both the beamforming vectors and the charging durations allocated to each IoT device are optimally determined; and (ii) **Random:** This benchmark considers a random spatial deployment of PBs, while still assuming access to PCSI for beamforming and scheduling.

It is important to highlight that the results were obtained via Monte Carlo simulations, considering 10^3 independent channel realizations across 10 different deployment scenarios. Unless stated otherwise, the simulation parameters used are those summarized in Table I.

To evaluate the performance of the proposed solution, Figure 2 illustrates the impact of the number of IoT devices (N) on the total system charging time (t_{T}). The results indicate that as N increases, the overall charging time also increases. However, this growth is not linear, primarily due to the ability of IoT devices to opportunistically harvest energy while neighboring devices are being actively charged. Furthermore, the results demonstrate the effectiveness of the proposed approach. Specifically, the suboptimal placement of PBs achieved through the proposed SOM-based strategy allows for a reduction of up to 87% in total charging time for $N = 50$ when compared to the Random benchmark, despite relying solely on SCSI. Additionally, the proposed method achieves performance levels that closely approximate those of the PCSI benchmark, thereby validating its practical applicability in real-world WET systems where acquiring perfect CSI is not feasible.

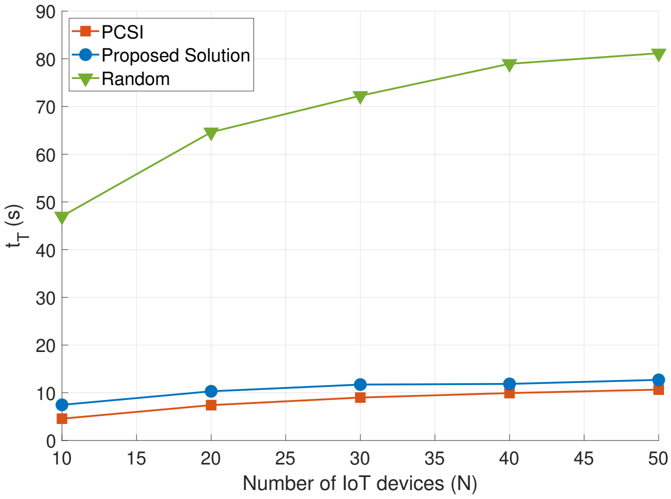

Fig. 2. Total charging time (t_{T}) versus N.

Figure 3 illustrates the impact of the number of antennas at the PBs (M) on the total charging time (t_{T}). The results reveal that increasing M leads to a slight reduction in t_{T}. This behavior can be attributed to the enhanced beamforming directivity achieved with a higher number of antennas, which, while improving energy harvested to the intended device, simultaneously reduces the energy opportunistically harvested by neighboring devices. These findings suggest that equipping PBs with a large number of antennas does not significantly enhance the overall efficiency of the WET system. Consequently, as demonstrated by the proposed solution, it is feasible to adopt simpler hardware architectures at the PBs if their locations are strategically optimized. Furthermore, the results confirm that the proposed solution consistently achieves substantial reductions in charging time across all evaluated values of M when compared to the Random benchmark, while maintaining performance levels close to the optimal benchmark. This validates the robustness and effectiveness of the proposed approach under varying system configurations.

Finally, it is important to evaluate the influence of the number of PBs on the system efficiency. Therefore, Table II illustrates the t_{T} for $K \in \{1, 2, 3, 4, 5, 6, 7\}$. From the results, it can be seen that the t_{T} decreases when K increases. Specifically, the initial addition of PBs leads to a substantial reduction in the total charging time, thereby enhancing the overall efficiency of the WET system. However, beyond a certain threshold, further increasing the number of PBs yields diminishing returns. This behavior can be attributed to the saturation effect inherent in the energy harvesting conversion process described in (5). Specifically, when the non-linear

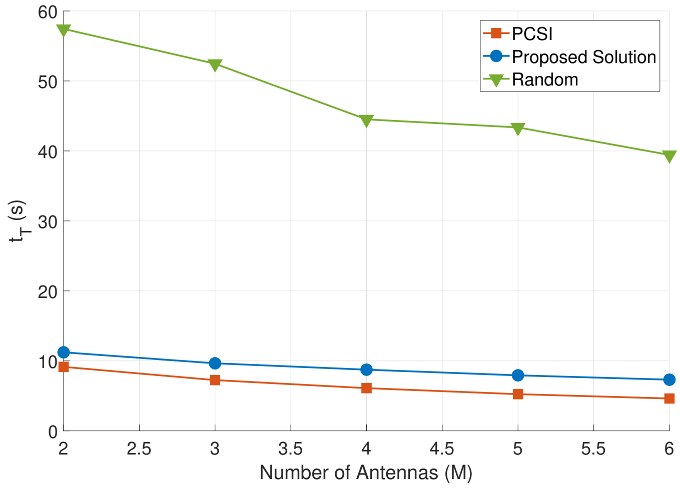

Fig. 3. Total charging time (t_{T}) versus M.

TABLE II
ANALYSIS OF THE INFLUENCE OF THE NUMBER OF PBS.

Number of PBs	Proposed Solution (T_{T})	Random (T_{T})
1	137.69	1084.77
2	50.46	381.58
3	31.06	195.82
4	18.94	145.87
5	15.31	96.22
6	11.94	73.95

characteristics of the EH devices are taken into account, increasing the input power beyond a certain threshold does not lead to a proportional increase in the harvested energy. Consequently, the results indicate that indefinitely increasing the number of PBs does not significantly improve system performance. This finding underscores the importance of intelligent PB placement, which not only enables the use of simpler hardware architectures without compromising efficiency but also reduces the required number of PBs, thereby simplifying the overall WET system design.

VI. CONCLUSION

This paper proposes an ML-based solution for jointly optimizing energy beamforming and PB placement in WET systems using only SCSI. By employing SOM and K-means clustering techniques, the method effectively reduces charging time by up to 87% and lowers hardware complexity through simplified analog beamforming. Results show that intelligent PBs placement is more impactful than simply increasing their number. The study demonstrates the potential of data-driven optimization for efficient and scalable WET system design. For future work, we aim to explore advanced PB placement strategies tailored for dynamic and complex environments, with a focus on enhancing adaptability and maintaining high system performance under varying deployment conditions.

REFERENCES

[1] A. Alabsi, A. Hawbani, X. Wang, A. Al-Dubai, J. Hu, S. A. Aziz, S. Kumar, L. Zhao, A. V. Shvetsov, and S. H. Alsamhi, “Wireless Power Transfer Technologies, Applications, and Future Trends: A Review,” *IEEE Transactions on Sustainable Computing*, vol. 10, no. 1, pp. 1–17, 2025.

[2] G. Moloudian, M. Hosseinifard, S. Kumar, R. B. V. B. Simorangkir, J. L. Buckley, C. Song, G. Fantoni, and B. O’Flynn, “RF Energy Harvesting Techniques for Battery-Less Wireless Sensing, Industry 4.0, and Internet of Things: A Review,” *IEEE Sensors Journal*, vol. 24, no. 5, pp. 5732–5745, 2024.

[3] O. A. López and H. Alves, *Wireless RF Energy Transfer in the Massive IoT Era: Towards Sustainable Zero-energy Networks*. Hoboken, New Jersey: John Wiley & Sons, 2022.

[4] O. M. Rosabal, O. L. A. Lopez, H. Alves, S. Montejo-Sanchez, and M. Latva-Aho, “On the Optimal Deployment of Power Beacons for Massive Wireless Energy Transfer,” *IEEE Internet of Things Journal*, vol. 8, no. 13, p. 10531–10542, Jul. 2021.

[5] D. Arivudainambi and S. Balaji, “Optimal Placement of Wireless Chargers in Rechargeable Sensor Networks,” *IEEE Sensors Journal*, vol. 18, no. 10, pp. 4212–4222, 2018.

[6] H. Dai, X. Wang, A. X. Liu, H. Ma, G. Chen, and W. Dou, “Wireless Charger Placement for Directional Charging,” *IEEE/ACM Transactions on Networking*, vol. 26, no. 4, pp. 1865–1878, 2018.

[7] A. Kumar and J. Singh, “Optimizing Location and Power of Chargers to Reduce Interference in Battery-Less WSNs,” *IEEE Sensors Journal*, vol. 24, no. 16, pp. 26 552–26 563, 2024.

[8] S. Zhang, C. Guo, T. Wang, and W. Zhang, “ON–OFF Analog Beamforming for Massive MIMO,” *IEEE Transactions on Vehicular Technology*, vol. 67, no. 5, pp. 4113–4123, 2018.

[9] M. Ahmed, R. Seraj, and S. M. S. Islam, “The k-means Algorithm: A Comprehensive Survey and Performance Evaluation,” *Electronics*, vol. 9, no. 8, 2020.

[10] E. Boshkovska, D. W. K. Ng, N. Zlatanov, and R. Schober, “Practical Non-Linear Energy Harvesting Model and Resource Allocation for SWIPT Systems,” *IEEE Communications Letters*, vol. 19, no. 12, pp. 2082–2085, 2015.

[11] Powercast, “Lifetime Power® Energy Harvesting Development Kit for Battery Recharging,” https://www.powercastco.com/p1110-eval-01-gate/, accessed: 2024-16-02.

[12] V. D. P. Souto, O. M. Rosabal, S. Montejo-Sánchez, O. L. A. López, H. Alves, and R. D. Souza, “An Analog Beamforming Strategy Based on Statistical Channel Information for Recharging Wireless Powered Sensor Networks,” *IEEE Sensors Journal*, vol. 24, no. 14, pp. 23 025–23 033, 2024.

[13] A. Guérin, P. Chauvet, and F. Saubion, “A survey on recent advances in self-organizing maps,” 2024. [Online]. Available: https://arxiv.org/abs/2501.08416

[14] T. Kohonen, “The self-organizing map,” *Proceedings of the IEEE*, vol. 78, no. 9, pp. 1464–1480, 1990.

[15] J. Wu, *Advances in K-means Clustering: A Data Mining Thinking*. Springer-Verlag Berlin Heidelberg, 2012.

[16] D. Arthur and S. Vassilvitskii, “k-means++: The advantages of careful seeding,” in *Proceedings of the 18th annual ACM-SIAM symposium on Discrete algorithms*. Society for Industrial and Applied Mathematics, 2007, pp. 1027–1035.

[17] O. L. A. López, S. Montejo-Sánchez, R. D. Souza, C. B. Papadias, and H. Alves, “On CSI-Free Multiantenna Schemes for Massive RF Wireless Energy Transfer,” *IEEE Internet of Things Journal*, vol. 8, no. 1, pp. 278–296, 2021.

[18] B. Clerckx, R. Zhang, R. Schober, D. W. K. Ng, D. I. Kim, and H. V. Poor, “Fundamentals of Wireless Information and Power Transfer: From RF Energy Harvester Models to Signal and System Designs,” *IEEE Journal on Selected Areas in Communications*, vol. 37, no. 1, pp. 4–33, 2019.